
Recurrent Highway Networks

Julian Georg Zilly*
ETH Zürich
jzilly@ethz.ch

Rupesh Kumar Srivastava* Jan Koutník Jürgen Schmidhuber
The Swiss AI Lab IDSIA / USI / SUPSI
{rupesh, hkou, juergen}@idsia.ch

Abstract

Many sequential processing tasks require complex nonlinear transition functions from one step to the next. However, recurrent neural networks with such “deep” transition functions remain difficult to train, even when using Long Short-Term Memory networks. We introduce a novel theoretical analysis of recurrent networks based on Geršgorin’s circle theorem that illuminates several modeling and optimization issues and improves our understanding of the LSTM cell. Based on this analysis we propose Recurrent Highway Networks, which are long not only in time but also in space, generalizing LSTMs to larger step-to-step depths. Experiments indicate that the proposed architecture results in complex but efficient models, beating previous models for character prediction on the Hutter Prize Wikipedia dataset and word-level language modeling on the Penn Treebank corpus.

1 Introduction & Previous Work

Network depth is of central importance in the resurgence of neural networks as a powerful machine learning paradigm [1]. Theoretical evidence indicates that deeper networks can be exponentially more efficient at representing certain function classes (see e.g. [2] and references therein). Due to their sequential nature, Recurrent Neural Networks (RNNs; 3–5) are deep *in time*. However, certain internal function mappings in RNNs usually do not take advantage of depth [6].

Unfortunately, increased depth represents a challenge when neural network parameters are optimized by means of error backpropagation [7–9]. Deep networks suffer from what are commonly referred to as the vanishing and exploding gradient problems [10–12], since the magnitude of the gradients may shrink or explode exponentially during backpropagation. These training difficulties were first studied in the context of standard RNNs where the depth through time is proportional to the length of input sequence, which may have arbitrary size. The widely used Long Short-Term Memory (LSTM; 13, 14) architecture was introduced to specifically address the problem of vanishing/exploding gradients for recurrent networks.

As the amount of available computational resources grows and complex learning problems are attacked, the vanishing gradient problem also becomes a limitation when training very deep feed-forward networks. The recently introduced *Highway Layers* [15] based on the LSTM cell address this limitation enabling the training of networks even with hundreds of stacked layers. These layers have been used to improve performance in speech recognition [16] and language modeling [17], and a variant of Highway networks called *Residual networks* is currently the state-of-the-art model for image recognition [18].

*These authors contributed equally.

In an attempt to add depth to the recurrent state transition in standard RNNs, Pascanu et al. [6] introduced Deep Transition RNNs (DT-RNNs) and Deep Transition RNNs with Skip connections (DT(S)-RNNs). While being powerful in principle, these architectures suffered from exacerbated gradient propagation issues. Due to this reason, deep state transitions for RNNs have not been widely adopted until now. A known way of creating large step-by-step depth is to let an RNN tick for several "micro time steps" per step of the sequence [19, 20]. However, then the RNN has to learn by itself which parameters to use for memories of previous events and which for standard deep nonlinear processing.

In this paper we first provide a new mathematical analysis of standard RNNs which offers a deeper understanding of various recurrent network architectures. Based on these insights, we introduce LSTM networks that are not only long in time but also long in space (per time step), and call them *Recurrent Highway Networks* or *RHNs*. They enable the use of substantially deeper transition architectures than have previously been trained while still maintaining successful backpropagation of the gradient. As a result, it becomes possible to construct powerful and trainable sequential models efficiently. Recurrent Highway Networks enable a powerful alternative method to make recurrent networks more expressive and complement other approaches such as stacking LSTM layers [21] or the more recent Grid-LSTMs [22].

2 Revisiting Gradient Flow in Recurrent Networks

Let \mathcal{L} denote the total loss for an input sequence of length T . Let $\mathbf{x}^{[t]} \in \mathbb{R}^m$ and $\mathbf{y}^{[t]} \in \mathbb{R}^n$ represent the output of a standard RNN at time t , $\mathbf{W} \in \mathbb{R}^{n \times m}$ and $\mathbf{R} \in \mathbb{R}^{n \times n}$ the input and recurrent weight matrices and $\mathbf{b} \in \mathbb{R}^n$ a bias vector. Then $\mathbf{y}^{[t]} = f(\mathbf{W}\mathbf{x}^{[t]} + \mathbf{R}\mathbf{y}^{[t-1]} + \mathbf{b})$ describes the dynamics of a standard RNN. The derivative of the loss \mathcal{L} with respect to parameters θ of a network can be expanded using the chain rule:

$$\frac{d\mathcal{L}}{d\theta} = \sum_{1 \leq t_2 \leq T} \frac{d\mathcal{L}^{[t_2]}}{d\theta} = \sum_{1 \leq t_2 \leq T} \sum_{1 \leq t_1 \leq t_2} \frac{\partial \mathcal{L}^{[t_2]}}{\partial \mathbf{y}^{[t_2]}} \frac{\partial \mathbf{y}^{[t_2]}}{\partial \mathbf{y}^{[t_1]}} \frac{\partial \mathbf{y}^{[t_1]}}{\partial \theta}. \quad (1)$$

The Jacobian matrix $\frac{\partial \mathbf{y}^{[t_2]}}{\partial \mathbf{y}^{[t_1]}}$, the key factor for the transport of the error from time step t_2 to time step t_1 , is obtained by chaining the derivatives across all time steps:

$$\frac{\partial \mathbf{y}^{[t_2]}}{\partial \mathbf{y}^{[t_1]}} := \prod_{t_1 < t \leq t_2} \frac{\partial \mathbf{y}^{[t]}}{\partial \mathbf{y}^{[t-1]}} = \prod_{t_1 < t \leq t_2} \mathbf{R}^\top \text{diag}[f'(\mathbf{R}\mathbf{y}^{[t-1]})], \quad (2)$$

where the input and bias have been omitted for simplicity. We can now obtain conditions for the gradients to vanish [10–12]. Let $\mathbf{A} := \frac{\partial \mathbf{y}^{[t]}}{\partial \mathbf{y}^{[t-1]}}$ define the temporal Jacobian, γ be a maximal bound on $f'(\mathbf{R}\mathbf{y}^{[t-1]})$ and σ_{max} be the largest singular value of \mathbf{R}^\top . Then the norm of the Jacobian satisfies:

$$\|\mathbf{A}\| \leq \|\mathbf{R}^\top\| \left\| \text{diag}[f'(\mathbf{R}\mathbf{y}^{[t-1]})] \right\| \leq \gamma \sigma_{max}, \quad (3)$$

which together with (2) provides the conditions for vanishing gradients ($\gamma \sigma_{max} < 1$). Note that γ depends on the activation function f , e.g. $|\tanh'(x)| \leq 1$, $|\sigma'(x)| \leq \frac{1}{4}$, $\forall x \in \mathbb{R}$, where σ is a logistic sigmoid. Similarly, we can show that if the spectral radius ρ of \mathbf{A} is greater than 1, exploding gradients will emerge since $\|\mathbf{A}\| \geq \rho$.

This description of the problem in terms of largest singular values or the spectral radius sheds light on boundary conditions for vanishing and exploding gradients yet does not illuminate how the eigenvalues are distributed overall. By applying the Geršgorin circle theorem we are able to provide further insight into the problem.

Geršgorin circle theorem (GCT) [23]: For any square matrix $\mathbf{A} \in \mathbb{R}^{n \times n}$,

$$\text{spec}(\mathbf{A}) \subset \bigcup_{i \in \{1, \dots, n\}} \left\{ \lambda \in \mathbb{C} \mid \|\lambda - a_{ii}\|_{\mathbb{C}} \leq \sum_{j=1, j \neq i}^n |a_{ij}| \right\}, \quad (4)$$

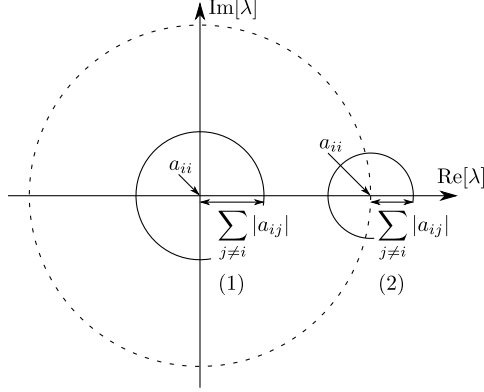


Figure 1: Illustration of the Geršgorin circle theorem. Two Geršgorin circles are centered around their diagonal entries a_{ii} . The corresponding eigenvalues lie within the radius of the sum of absolute values of non-diagonal entries a_{ij} . Circle (1) represents an exemplar Geršgorin circle for an RNN initialized with small random values. Circle (2) represents the same for an RNN with identity initialization of the diagonal entries of the recurrent matrix and small random values otherwise. The dashed circle denotes the unit circle of radius 1.

i.e., the eigenvalues of matrix \mathbf{A} , comprising the spectrum of \mathbf{A} , are located within the union of the complex circles centered around the diagonal values a_{ii} of \mathbf{A} with radius $\sum_{j=1, j \neq i}^n |a_{ij}|$ equal to the sum of the absolute values of the non-diagonal entries in each row of \mathbf{A} . Two example Geršgorin circles referring to differently initialized RNNs are depicted in Figure 1.

Using GCT we can understand the relationship between the entries of \mathbf{R} and the possible locations of the eigenvalues of the Jacobian. Shifting the diagonal values a_{ii} shifts the possible locations of eigenvalues. Having large off-diagonal entries will allow for a large spread of eigenvalues. Small off-diagonal entries yield smaller radii and thus a more confined distribution of eigenvalues around the diagonal entries a_{ii} .

Let us assume that matrix \mathbf{R} is initialized with a zero-mean Gaussian distribution. We can then infer the following:

- If the values of \mathbf{R} are initialized with a standard deviation close to 0, then the spectrum of \mathbf{A} , which is largely dependent on \mathbf{R} , is also initially centered around 0. An example of a Geršgorin circle that could then be corresponding to a row of \mathbf{A} is circle (1) in Figure 1. The magnitude of most of \mathbf{A} 's eigenvalues $|\lambda_i|$ are initially likely to be substantially smaller than 1. Additionally, employing the commonly used L_1/L_2 weight regularization will also limit the magnitude of the eigenvalues.
- Alternatively, if entries of \mathbf{R} are initialized with a large standard deviation, the radii of the Geršgorin circles corresponding to \mathbf{A} increase. Hence, \mathbf{A} 's spectrum may possess eigenvalues with norms greater 1 resulting in exploding gradients. As the radii are summed over the size of the matrix, larger matrices will have an associated larger circle radius. In consequence, larger matrices should be initialized with correspondingly smaller standard deviations to avoid exploding gradients.

Le et al. [24] proposed to initialize \mathbf{R} with identity and small random values on the off-diagonals. This changes the situation depicted by GCT – the result of the identity initialization is indicated by circle (2) in Figure 1. Initially, since $a_{ii} = 1$, the spectrum described in GCT is centered around 1, ensuring that gradients are less likely to vanish. However, this is not a flexible remedy. During training some eigenvalues can easily become larger than one, resulting in exploding gradients. We conjecture that due to this reason, extremely small learning rates were used by Le et al. [24]. Most importantly, unlike variants of LSTM, other RNNs have no direct mechanism to rapidly regulate their Jacobian eigenvalues *across time steps*, which can be efficient and necessary for complex sequence processing.

3 Recurrent Highway Networks (RHN)

Highway layers [25] enable easy training of very deep feedforward networks through the use of adaptive computation. Let $\mathbf{h} = H(\mathbf{x}, \mathbf{W}_H)$, $\mathbf{t} = T(\mathbf{x}, \mathbf{W}_T)$, $\mathbf{c} = C(\mathbf{x}, \mathbf{W}_C)$ be outputs of nonlinear transforms H, T and C with associated weight matrices (including biases) $\mathbf{W}_{H,T,C}$. T and C typically utilize a sigmoid (σ) nonlinearity and are referred to as the *transform* and the *carry* gates since they regulate the passing of the *transformed* input via H or the *carrying* over of the original input \mathbf{x} . The Highway layer computation is defined as

$$\mathbf{y} = \mathbf{h} \cdot \mathbf{t} + \mathbf{x} \cdot \mathbf{c}, \quad (5)$$

where " \cdot " denotes element-wise multiplication.

Recall that the recurrent state transition in a standard RNN is described by $\mathbf{y}^{[t]} = f(\mathbf{W}\mathbf{x}^{[t]} + \mathbf{R}\mathbf{y}^{[t-1]} + \mathbf{b})$. We propose to construct a Recurrent Highway Network (RHN) layer with one or multiple Highway layers in the recurrent state transition. The number of layers in the recurrent state transition will in the following be referred to as *recurrence depth*. Formally, let $\mathbf{W}_{H,T,C} \in \mathbb{R}^{n \times m}$ and $\mathbf{R}_{H_\ell, T_\ell, C_\ell} \in \mathbb{R}^{n \times n}$ represent the weights matrices of the H nonlinear transform and the T and C gates at layer $\ell \in \{1, \dots, L\}$. The biases are denoted by $\mathbf{b}_{H_\ell, T_\ell, C_\ell} \in \mathbb{R}^n$ and let \mathbf{s}_ℓ denote the intermediate output at layer ℓ with $\mathbf{s}_0^{[t]} = \mathbf{y}^{[t-1]}$. Then an RHN layer with a *recurrence depth* of L is described by

$$\mathbf{s}_\ell^{[t]} = \mathbf{h}_\ell^{[t]} \cdot \mathbf{t}_\ell^{[t]} + \mathbf{s}_{\ell-1}^{[t]} \cdot \mathbf{c}_\ell^{[t]}, \quad (6)$$

where

$$\mathbf{h}_\ell^{[t]} = \tanh(\mathbf{W}_H \mathbf{x}^{[t]} \mathbb{I}_{\{\ell=1\}} + \mathbf{R}_{H_\ell} \mathbf{s}_{\ell-1}^{[t]} + \mathbf{b}_{H_\ell}), \quad (7)$$

$$\mathbf{t}_\ell^{[t]} = \sigma(\mathbf{W}_T \mathbf{x}^{[t]} \mathbb{I}_{\{\ell=1\}} + \mathbf{R}_{T_\ell} \mathbf{s}_{\ell-1}^{[t]} + \mathbf{b}_{T_\ell}), \quad (8)$$

$$\mathbf{c}_\ell^{[t]} = \sigma(\mathbf{W}_C \mathbf{x}^{[t]} \mathbb{I}_{\{\ell=1\}} + \mathbf{R}_{C_\ell} \mathbf{s}_{\ell-1}^{[t]} + \mathbf{b}_{C_\ell}), \quad (9)$$

and $\mathbb{I}_{\{\cdot\}}$ is the indicator function.

A schematic illustration of the RHN computation graph is shown in Figure 2. The output of the RHN layer is the output of the L^{th} Highway layer i.e. $\mathbf{y}^{[t]} = \mathbf{s}_L^{[t]}$.

Note that $\mathbf{x}^{[t]}$ is directly transformed only by the first Highway layer ($\ell = 1$) in the recurrent transition¹ and for this layer $\mathbf{s}_{\ell-1}^{[t]}$ is the RHN layer's output of the previous time step, or again concisely $\mathbf{s}_0^{[t]} = \mathbf{y}^{[t-1]}$. Subsequent Highway layers only process the outputs of the previous ones. Dotted vertical lines in Figure 2 separate multiple Highway layers in the recurrent transition.

For conceptual clarity, it is important to observe that an RHN layer with $L = 1$ is essentially a basic variant of an LSTM layer. Similar to other variants such as GRU [26] and those studied by Greff et al. [27] and Jozefowicz et al. [28], it retains the essential components of the LSTM – multiplicative gating units controlling the flow of information through self-connected additive cells. However, an RHN layer naturally extends to $L > 1$, extending the LSTM to model far more complex state transitions. Like Highway and LSTM layers, other variants can also be constructed without changing the basic principles, for example by fixing one or both of the gates to always be *open*, or coupling the gates as done for the experiments in this paper.

The simpler formulation of RHN layers allows an analysis similar to standard RNNs based on GCT. Omitting the inputs and biases, the temporal Jacobian for an RHN layer with recurrence depth of 1 (such that $\mathbf{y}^{[t]} = \mathbf{h}^{[t]} \cdot \mathbf{t}^{[t]} + \mathbf{y}^{[t-1]} \cdot \mathbf{c}^{[t]}$) is

$$\mathbf{A} := \frac{\partial \mathbf{y}^{[t]}}{\partial \mathbf{y}^{[t-1]}} = \text{diag}(\mathbf{c}^{[t]}) + \mathbf{H}' \text{diag}(\mathbf{t}^{[t]}) + \mathbf{C}' \text{diag}(\mathbf{y}^{[t-1]}) + \mathbf{T}' \text{diag}(\mathbf{h}^{[t]}), \quad (10)$$

¹This is not strictly necessary, but simply a convenient choice.

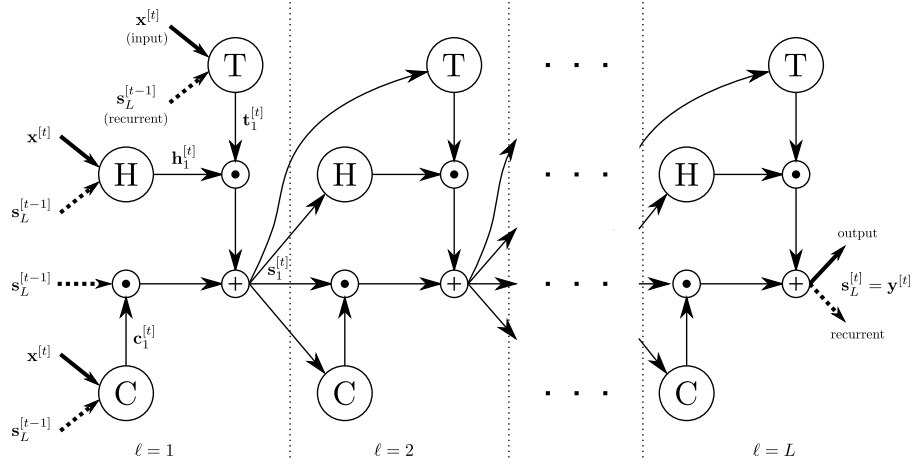


Figure 2: Schematic showing computation within an RHN layer inside the recurrent loop. Vertical dashed lines delimit stacked Highway layers. Horizontal dashed lines imply the extension of the recurrence depth by stacking further layers. H, T & C are the transformations described in equations 7, 8 and 9, respectively.

where

$$\mathbf{H}' = \mathbf{R}_H^\top \text{diag}[\tanh'(\mathbf{R}_H \mathbf{y}^{[t-1]})], \quad (11)$$

$$\mathbf{T}' = \mathbf{R}_T^\top \text{diag}[\sigma'(\mathbf{R}_T \mathbf{y}^{[t-1]})], \quad (12)$$

$$\mathbf{C}' = \mathbf{R}_C^\top \text{diag}[\sigma'(\mathbf{R}_C \mathbf{y}^{[t-1]})], \quad (13)$$

and has a spectrum of:

$$\begin{aligned} \text{spec}(\mathbf{A}) \subset \bigcup_{i \in \{1, \dots, n\}} \left\{ \lambda \in \mathbb{C} \mid \left\| \lambda - \mathbf{c}_i^{[t]} - \mathbf{H}'_{ii} \mathbf{t}_i^{[t]} - \mathbf{C}'_{ii} \mathbf{y}_i^{[t-1]} - \mathbf{T}'_{ii} \mathbf{h}_i^{[t]} \right\|_{\mathbf{C}} \right. \\ \left. \leq \sum_{j=1, j \neq i}^n \left| \mathbf{H}'_{ij} \mathbf{t}_j^{[t]} + \mathbf{C}'_{ij} \mathbf{y}_j^{[t-1]} + \mathbf{T}'_{ij} \mathbf{h}_j^{[t]} \right| \right\}. \end{aligned} \quad (14)$$

Equation 14 captures the influence of the gates on the eigenvalues of \mathbf{A} . Compared to the situation for standard RNN, it can be seen that an RHN layer has more flexibility in adjusting the centers and radii of the Geršgorin circles. In particular, two limiting cases can be noted. If all carry gates are fully open and transform gates are fully closed, we have $\mathbf{c} = \mathbf{1}_n$, $\mathbf{t} = \mathbf{0}_n$ and $\mathbf{T}' = \mathbf{C}' = \mathbf{0}_{n \times n}$ (since σ is saturated). This results in

$$\mathbf{c} = \mathbf{1}_n, \quad \mathbf{t} = \mathbf{0}_n \Rightarrow \lambda_i = 1 \quad \forall i \in \{1, \dots, n\}, \quad (15)$$

i.e. all eigenvalues are set to 1 since the Geršgorin circle radius is shrunk to 0 and each diagonal entry is set to $\mathbf{c}_i = 1$. In the other limiting case, if $\mathbf{c} = \mathbf{0}_n$ and $\mathbf{t} = \mathbf{1}_n$ then the eigenvalues are simply those of \mathbf{H}' . As the gates vary between 0 and 1, each of the eigenvalues of \mathbf{A} can be dynamically adjusted to any combination of the above limiting behaviors.

The key takeaways from the above analysis are as follows. Firstly, GCT allows us to observe the behavior of the full spectrum of the temporal Jacobian, and the effect of gating units on it. We expect that for learning multiple temporal dependencies from real-world data efficiently, *it is not sufficient to avoid vanishing and exploding gradients*. The gates in RHN layers provide a more versatile setup for *dynamically* remembering, forgetting and transforming information compared to standard RNNs. Secondly, based on the above observations it becomes reasonable to expect that certain sequential problems require a capacity to express complicated gating functions to rapidly regulate information flow. Depth is a widely used method to add such expression to functions, motivating us to use multiple layers of H , T and C transformations. In this paper we opt for extending RHN layers to $L > 1$ using Highway layers in favor of simplicity and ease of training. However, we expect that in some cases

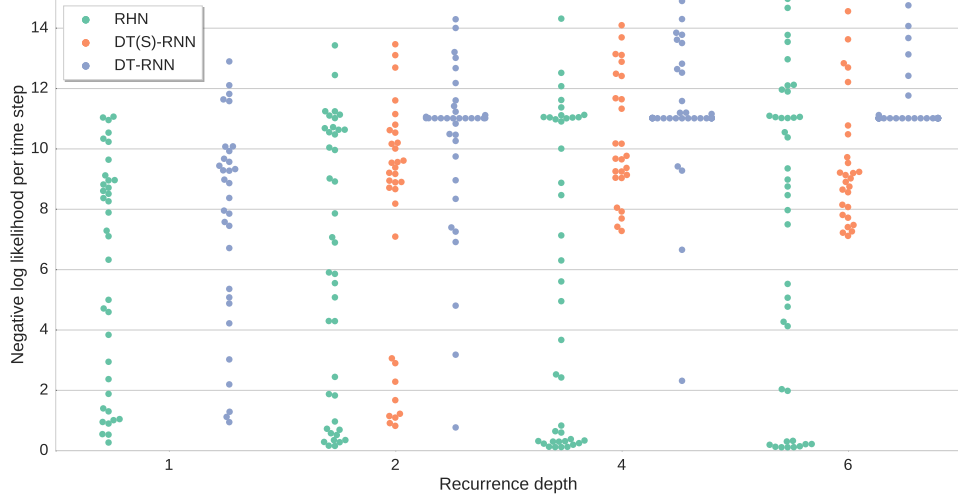


Figure 3: Swarm plot of optimization experiment results for various architectures for different depths on next step prediction on the JSB Chorales dataset. Each point is the result of optimization using a random hyperparameter setting. The number of network parameters increases with depth, but is kept the same across architectures for each depth. For architectures other than RHN, the random search was unable to find good hyperparameters when depth increased.

stacking plain layers for these transformations can also be useful. Finally, the analysis of the RHN layer’s flexibility in controlling its spectrum furthers our theoretical understanding of LSTM and Highway networks and their variants. For feedforward Highway networks, the Jacobian of the layer transformation ($\partial \mathbf{y} / \partial \mathbf{x}$) takes place of the temporal Jacobian in the above analysis. We can then observe that each Highway layer allows increased flexibility in controlling how various components of the input get transformed or carried. This flexibility is the likely reason behind the performance improvement from Highway layers even in cases where network depth is not high [17].

4 Experiments

In this work, the carry gate was coupled to the transform gate by setting $C(\cdot) = \mathbf{1}_n - T(\cdot)$ similar to the suggestion for Highway networks. This coupling is also used by the GRU recurrent architecture. It reduces model size for a fixed number of units and prevents an unbounded blow-up of state values leading to more stable training, but imposes a modeling bias which may be sub-optimal for certain tasks [27, 28]. An output non-linearity similar to LSTM networks could alternatively be used to combat this issue. For optimization and Wikipedia experiments, we bias the transform gates towards being closed at the start of training. All networks use a single hidden RHN layer since we are only interested in studying the effect of recurrence depth, and not of stacking multiple layers, which is already known to be useful. Detailed configurations for all experiments are included in the supplementary material. Code and results database for the experiments will be publicly released in the near future.

4.1 Optimization

RHN is an architecture designed to enable the optimization of recurrent networks with deep transitions. Therefore, the primary experimental verification we seek is whether RHNs with higher recurrence depth are easier to optimize compared to other alternatives, preferably using simple gradient based methods.

We compare optimization of RHNs to DT-RNNs and DT(S)-RNNs [6]. Networks with recurrence depth of 1, 2, 4 and 6 are trained for next step prediction on the JSB Chorales polyphonic music prediction dataset [29]. Network sizes are chosen such that the total number of network parameters increases as the recurrence depth increases, but remains same across architectures. A hyperparameter search is then conducted for SGD-based optimization of each architecture and depth combination for

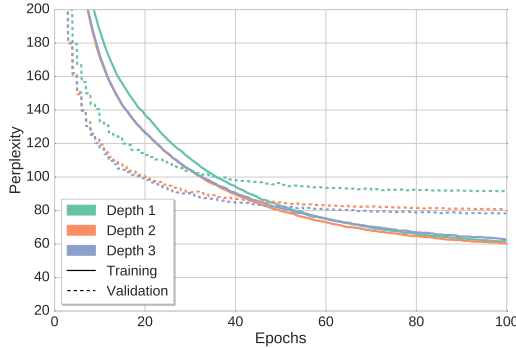


Figure 4: Training and Validation set perplexity over the course of training on Penn Treebank word-level language modeling using RHNs with fixed parameter budget and increasing recurrence depth.

Table 1: Bits per character (BPC) on the Hutter Wikipedia dataset (without dynamic evaluation).

Architecture	BPC	# Param.	Test Data
Stacked LSTM [21]	1.67	27.0 M	last 4 MB
GF-RNN [35]	1.58	20.0 M	last 5 MB
Grid-LSTM [22]	1.47	16.8 M	last 5 MB
RHN	1.42	8.0 M	last 5 MB

Table 2: Validation and test set perplexity for different recurrence depths while keeping the number of parameters fixed to 31.25 M.

Rec. Depth	Best Val.	Test
1	91.45	92.08
2	80.72	81.28
3	78.28	79.34

fair comparisons. In the absence of optimization difficulties, larger networks should reach a similar or better loss value compared to smaller networks. However, the swarm plot in Figure 3 shows that both DT-RNN and DT(S)-RNN get considerably harder to optimize with increasing depth. Increasing the recurrence depth does not adversely affect optimization of RHNs. These results are similar to those obtained in an optimization study on feedforward Highway networks [25].

4.2 Sequence Modeling

Wikipedia: We train an RHN with recurrence depth of 5 and 864 units on the challenging Hutter Prize Wikipedia dataset (enwik8) [30]. The task is next symbol prediction with 205 unicode symbols in total. Training is performed using SGD with momentum and weight noise as used by Graves [31]. Due to its size (100 M characters in total) and complexity (inclusion of Latin/non-Latin alphabets, XML markup and various special characters) this dataset allows us to stress the learning and generalization capacity of RHNs. The previous best result for this task was obtained using a 6-layer Grid-LSTM [22] with tied weights. The RHN outperforms it using less than half the parameters, fewer units per layer and no weight-tying, demonstrating that adding depth to the recurrent transition efficiently utilizes parameters to improve model capacity. Table 1 compares our result to previous models.

Penn Treebank: To examine the effect of recurrence depth we trained RHNs with one RHN layer and fixed total parameters (31.25 M) but with recurrence depths of 1, 2 and 3 for word level language modeling on the Penn TreeBank dataset [32]. We use variational dropout regularization introduced by Gal [33], who obtained the best single model result on this task (75.0/73.4 perplexity on the test set without/with MC testing) using a network with two LSTM layers and 66 M total parameters. Figure 4 shows the progress of training and validation set perplexity for each depth. Best scores obtained on validation set and corresponding test set scores are shown in Table 2. The lowest value reached for both scores improves as the recurrence depth increases for a fixed parameter budget, demonstrating that deep transitions can be used to obtain improved performance even on small scale datasets.

For the above experiments, the dropout probabilities were kept the same as in the work by Gal, who tuned them for the LSTM architecture of [34]. We further tuned the dropout probabilities on the validation set for an RHN with recurrence depth of 5 (1000 units per highway layer, ≈ 32 M parameters) and obtained validation/test perplexity of **72.8/71.3 without using MC testing**. Table 3 compares our result with the best recent single model results in the literature. For comparison, the best result using an ensemble of models on this dataset is 68.7 [33, 34].

Table 3: Single model validation and test perplexity of recent state of the art word-level language models on the Penn Treebank dataset. The model from Kim et al. [17] uses feedforward highway layers to transform a character-aware word representation before feeding it into LSTM layers. *dropout* indicates the regularization used by Zaremba et al. [34] which was applied to only the input and output of recurrent layers. *Variational* refers to the dropout regularization from Gal [33] based on a probabilistic interpretation of the models. MC refers to testing using 1000 samples at test time. An RHN with 5 highway layers comfortably outperforms all previous single model results.

Model	Size	Best Val.	Test
Conv.+Highway+LSTM+dropout [17]	19 M	–	78.9
Variational LSTM+MC [33]	20 M	–	78.6
LSTM+dropout [34]	66 M	82.2	78.4
Variational LSTM [33]	66 M	77.3	75.0
Variational LSTM+MC [33]	66 M	–	73.4
Variational RHN	32 M	72.8	71.3

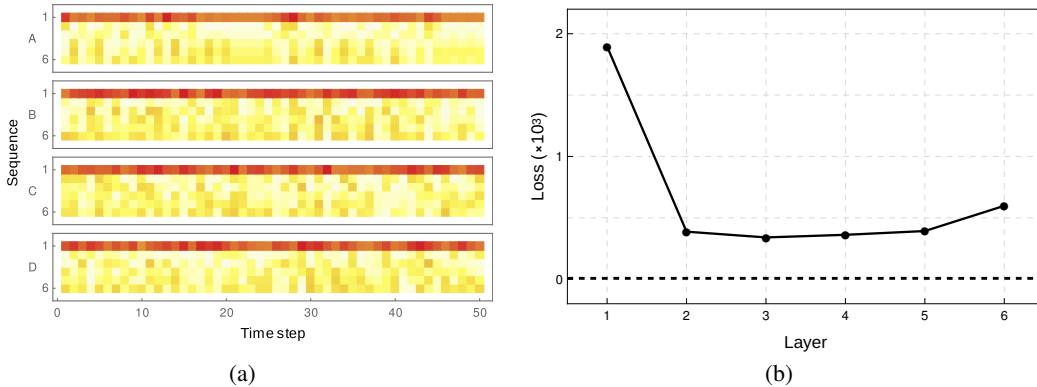


Figure 5: (a) Activations of the transform (T) gates for different recurrence depths in 4 different sequences. An active transform gate indicates that the recurrence layer is used to process input at a particular time step, as opposed to passing it to the next layer. (b) Changes in loss when the recurrence layers are biased towards carry behavior (effectively removed), one layer at a time.

5 Analysis

We analyze the inner workings of RHNs through inspection of gate activations, and their effect on network performance. For the RHN with 6-layered recurrence optimized on the JSB Chorales dataset (subsection 4.1), Figure 5(a) shows the mean transform gate activity in each layer over time steps for 4 example sequences. We note that while the gates are biased towards zero (white) at initialization, all layers are utilized in the trained network. The gate activity in the first layer of the recurrent transition is typically high on average, indicating that at least one layer of recurrent transition is almost always utilized. Gates in other layers have varied behavior, dynamically switching their activity over time in a different way for each sequence.

The contributions of the layers towards network performance can be quantified through a *lesioning* experiment similar to that introduced by Srivastava et al. [25]. For one layer at a time, all the gates are pushed towards carry behavior by setting the bias to a large negative value, and the resulting loss is measured. Figure 5(b) shows the change in loss due to the biasing of each layer, and hence its contribution to the network performance. In this case, we find that the first layer contributes several times more to the overall performance compared to others. It is notable that removing any layer hurts the performance substantially due to the recurrent nature of the network.

6 Conclusion

We developed a new analysis of the behavior of RNNs based on the Geršgorin Circle Theorem. The analysis provides insights into other recently proposed architectures such as IRNNs and Highway networks. A main result is the showcasing of inherent limitations of RNNs and the ability of gates to variably influence learning. Furthermore, we introduced *Recurrent Highway Networks*, a powerful new model designed to take advantage of increased depth in the recurrent transition, without incurring additional training problems. Experiments confirmed the theoretical optimization advantages as well as improved performance on sequence modeling tasks due to increased recurrence depth. Future work will compare RHN to a pure LSTM with several micro-ticks per time step.

Acknowledgements: This research was partially supported by the H2020 project “Intuitive Natural Prosthesis Utilization” (INPUT; #687795) and SNSF grant “Advanced Reinforcement Learning” (#156682). We thank Klaus Greff, Sjoerd van Steenkiste and Bas Steunebrink for many insightful discussions. The Brainstorm [36] library was used for all experiments excluding those on Penn Treebank, for which we modified the Torch7 [37] code provided by Gal [33].

References

- [1] Jürgen Schmidhuber. Deep learning in neural networks: An overview. *Neural Networks*, 61:85–117, 2015.
- [2] Monica Bianchini and Franco Scarselli. On the complexity of neural network classifiers: A comparison between shallow and deep architectures. *IEEE Transactions on Neural Networks*, 2014.
- [3] A. J. Robinson and F. Fallside. The utility driven dynamic error propagation network. Technical Report CUED/F-INFENG/TR.1, Cambridge University Engineering Department, 1987.
- [4] Paul J Werbos. Generalization of backpropagation with application to a recurrent gas market model. *Neural Networks*, 1(4):339–356, 1988.
- [5] R. J. Williams. Complexity of exact gradient computation algorithms for recurrent neural networks. Technical Report NU-CCS-89-27, Boston: Northeastern University, College of Computer Science, 1989.
- [6] R. Pascanu, C. Gulcehre, K. Cho, and Y. Bengio. How to construct deep recurrent neural networks. *ArXiv e-prints*, December 2013.
- [7] S. Linnainmaa. The representation of the cumulative rounding error of an algorithm as a taylor expansion of the local rounding errors. Master’s thesis, Univ. Helsinki, 1970.
- [8] Seppo Linnainmaa. Taylor expansion of the accumulated rounding error. *BIT Numerical Mathematics*, 16(2):146–160, 1976. ISSN 1572-9125.
- [9] Paul J. Werbos. *System Modeling and Optimization: Proceedings of the 10th IFIP Conference New York City, USA, August 31 – September 4, 1981*, chapter Applications of advances in nonlinear sensitivity analysis, pages 762–770. Springer Berlin Heidelberg, 1982.
- [10] S Hochreiter. Untersuchungen zu dynamischen neuronalen Netzen. Master’s thesis, Institut f. Informatik, Technische Univ. Munich, 1991.
- [11] S. Hochreiter, Y. Bengio, P. Frasconi, and J. Schmidhuber. Gradient flow in recurrent nets: the difficulty of learning long-term dependencies. In S. C. Kremer and J. F. Kolen, editors, *A Field Guide to Dynamical Recurrent Neural Networks*. IEEE Press, 2001.
- [12] R. Pascanu, T. Mikolov, and Y. Bengio. On the difficulty of training recurrent neural networks. *ArXiv e-prints*, November 2012.
- [13] S. Hochreiter and J. Schmidhuber. Long short-term memory. *Neural Computation*, 9(8):1735–1780, 1997.
- [14] Felix A. Gers, Jürgen Schmidhuber, and Fred Cummins. Learning to forget: Continual prediction with lstm. *Neural Computation*, 12(10):2451–2471, 2016/02/18 2000.
- [15] Rupesh Kumar Srivastava, Klaus Greff, and Jürgen Schmidhuber. Highway networks. *arXiv preprint arXiv:1505.00387*, 2015.
- [16] Yu Zhang, Guoguo Chen, Dong Yu, Kaisheng Yaco, Sanjeev Khudanpur, and James Glass. Highway long short-term memory RNNs for distant speech recognition. In *2016 IEEE, ICASSP*, 2016.

- [17] Yoon Kim, Yacine Jernite, David Sontag, and Alexander M Rush. Character-aware neural language models. *arXiv preprint arXiv:1508.06615*, 2015.
- [18] K. He, X. Zhang, S. Ren, and J. Sun. Deep residual learning for image recognition. *arXiv preprint arXiv:1512.03385*, 2015.
- [19] A. Graves. Adaptive Computation Time for Recurrent Neural Networks. *ArXiv e-prints*, March 2016.
- [20] Jürgen Schmidhuber. Reinforcement learning in markovian and non-markovian environments. In *Advances in Neural Information Processing Systems 3*. Morgan-Kaufmann, 1991.
- [21] S. Fernandez, A. Graves, and J. Schmidhuber. Sequence labelling in structured domains with hierarchical recurrent neural networks. In *Proceedings of the 20th International Joint Conference on Artificial Intelligence (IJCAI)*, 2007.
- [22] Nal Kalchbrenner, Ivo Danihelka, and Alex Graves. Grid long short-term memory. *CoRR*, abs/1507.01526, 2015. URL <http://arxiv.org/abs/1507.01526>.
- [23] S. Geršgorin. Über die Abgrenzung der Eigenwerte einer Matrix. *Bulletin de l'Académie des Sciences de l'URSS. Classe des sciences mathématiques*, no. 6:749–754, 1931.
- [24] Q. V. Le, N. Jaitly, and G. E. Hinton. A Simple Way to Initialize Recurrent Networks of Rectified Linear Units. *ArXiv e-prints*, April 2015.
- [25] Rupesh K Srivastava, Klaus Greff, and Juergen Schmidhuber. Training very deep networks. In *Advances in Neural Information Processing Systems 28*, pages 2368–2376. Curran Associates, Inc., 2015.
- [26] Kyunghyun Cho, Bart Van Merriënboer, Caglar Gulcehre, Dzmitry Bahdanau, Fethi Bougares, Holger Schwenk, and Yoshua Bengio. Learning phrase representations using rnn encoder-decoder for statistical machine translation. *arXiv preprint arXiv:1406.1078*, 2014.
- [27] K. Greff, R. K. Srivastava, J. Koutník, B. R Steunebrink, and J. Schmidhuber. LSTM: A Search Space Odyssey. *arXiv preprint arXiv:1503.04069*, 2015.
- [28] Rafal Jozefowicz, Wojciech Zaremba, and Ilya Sutskever. An empirical exploration of recurrent network architectures. 2015.
- [29] N. Boulanger-Lewandowski, Y. Bengio, and P. Vincent. Modeling temporal dependencies in high-dimensional sequences: Application to polyphonic music generation and transcription. *ArXiv e-prints*, June 2012.
- [30] M. Hutter. The human knowledge compression contest. <http://prize.hutter1.net/>, 2012.
- [31] A. Graves. Generating sequences with recurrent neural networks. *ArXiv e-prints*, August 2013.
- [32] Mitchell P. Marcus, Mary Ann Marcinkiewicz, and Beatrice Santorini. Building a large annotated corpus of english: The penn treebank. *Comput. Linguist.*, 19(2):313–330, June 1993. ISSN 0891-2017.
- [33] Yarín Gal. A theoretically grounded application of dropout in recurrent neural networks. *arXiv preprint arXiv:1512.05287*, 2015.
- [34] W. Zaremba, I. Sutskever, and O. Vinyals. Recurrent Neural Network Regularization. *ArXiv e-prints*, September 2014.
- [35] Junyoung Chung, Caglar Gulcehre, Kyunghyun Cho, and Yoshua Bengio. Gated feedback recurrent neural networks. In *International Conference on Machine Learning*, 2015.
- [36] Klaus Greff, Rupesh Kumar Srivastava, and Jürgen Schmidhuber. Brainstorm: Fast, Flexible and Fun Neural Networks, Version 0.5, 2015. URL <https://github.com/IDSIA/brainstorm>.
- [37] Ronan Collobert, Koray Kavukcuoglu, and Clément Farabet. Torch7: A matlab-like environment for machine learning. In *BigLearn, NIPS Workshop*, 2011.
- [38] Alex Graves. Practical variational inference for neural networks. In *Advances in Neural Information Processing Systems 24*, pages 2348–2356. Curran Associates, Inc., 2011.

7 Supplementary Material

7.1 Details of Experimental Setups

Optimization

In these experiments, we compare RHNs to Deep Transition RNNs (DT-RNNs) and Deep Transition RNNs with Skip connections (DT(S)-RNNs) introduced by [6]. A total number of 60 runs per architecture and depth is recorded. The number of units in each layer of the recurrence is fixed to $\{1.5 \times 10^5, 3 \times 10^5, 6 \times 10^5, 9 \times 10^5\}$ for recurrence depths of 1, 2, 4 and 6, respectively. The batch size is set to 32. The $\tanh(\cdot)$ is used as the activation function for the nonlinear layers. A maximum of 1000 epochs with stopping after 100 epochs without improvement are specified. Random search is conducted sampling the initial transform gate bias from $\{0, -1, -2, -3\}$. The initial learning rate is sampled uniformly (on logarithmic scale) between 10^0 and 10^{-4} . Finally, all weights are initialized with a Gaussian distribution with standard deviation sampled uniformly (on logarithmic scale) from 10^{-2} to 10^{-8} . For these experiments, optimization was performed using stochastic gradient descent with momentum, where momentum was set to 0.9.

Wikipedia

The Wikipedia dataset, created by Hutter [30], is split into sequences of length 50 as done by Graves in [31]. This dataset incorporates clear long-term dependencies introduced through the HTML-language the data is presented in.

We trained an RHN with 5 stacked layers in the recurrent state transition with 864 units, creating a network with a total of 8 million parameters to demonstrate the increased capacity the stacking of Highway layers in the recurrence of an RNN may offer. A constant learning rate of 0.001 with momentum of 0.9 and batch size 100 was used. A very weak L_2 -weight decay of $1e-6$ was applied. Crucially for training, the activation of the previous sequence, each of length 50, was kept to enable learning of very long-term dependencies as done in [31]. Without this context, long-term dependencies are extremely hard to learn. Additive Gaussian weight noise [38] was added to prevent overfitting and iteratively increased to 0.03 in increments of 0.01. When training did not continue to improve the training loss, the learning rate was divided by a factor of 2.

Penn Treebank

The Penn Treebank text corpus [32] is a comparatively small standard benchmark in language modeling. The setup of the data and most of the code is based on Gal’s [33] extension of Zaremba’s [34] public LSTM dropout code. Principally only the LSTM model was substituted by an RHN model. To showcase the influence of recurrence depth, we trained and compared RHNs with 1 layer and recurrence depth of $\{1, 2, 3\}$ with a total budget of 31.25 M parameters. This leads to RHN sizes of 1250, 1159, and 1089, respectively. Regularization of recurrent networks using variational dropout by Gal [33] was applied to 1 RHN layer, batch size 20, sequence length 50, learning rate of 0.2, learning rate decay of 1.03 which started after 20 epochs, weight decay of $1e-7$ and a maximum gradient norm of 10. Dropout rates were chosen to be 0.3 for the embedding layer, 0.5 for the input to the gates, 0.3 for the hidden units and 0.5 for the output activations. All weights were initialized from a uniform distribution between $[-0.04, 0.04]$.

To demonstrate that RHNs perform well even on smaller datasets by achieving state-of-the-art results as shown in table 3, the hyper parameters were further tuned. For this run, the initial learning rate was set to 0.2, learning rate decay to 1.02 starting after 20 epochs, sequence length to 35, number of units to 1000, number of RHN layers to 1 while recurrence depth was set to 5. Furthermore, the maximal gradient norm limit was set to 10, weight decay to $1e-7$, batch size to 20 and initial weights were again uniformly sampled between $[-0.04, 0.04]$. Regarding variational dropout, a rate of 0.25 was applied to both the embedding and hidden units and a rate of 0.7 was applied to both input to gates and output of the network.